NILU
TECHNICAL REPORT NO.:10/1983
REFERENCE: N-8218
DATE: NOVEMBER 1983

OZONE IN THE TROPOSPHERE

by

Øystein Hov

NORWEGIAN INSTITUTE FOR AIR RESEARCH
P.O.BOX 130, N-2001 LILLESTRØM
NORWAY

OZONE IN THE TROPOSPHERE

1 INTRODUCTION

Most of the solar utraviolet radiation is absorbed by stratospheric ozone before it reaches the troposphere, where approximately 10% of the atmospheric content of ozone is found. The research on the distribution formation and destruction of atmospheric ozone has been focused on the stratosphere. For a long time, ozone in the troposphere was considered to be chemically nearly inert, reflecting the balance between stratospheric intrusion and surface removal (1). Junge found that within the Northern Hemisphere, representative data of tropospheric ozone have a uniform seasonal variation, the phase of which is delayed by about two months with respect to the injection into the troposphere. He suggested that this delay was controlled by the rate of destruction of ozone within the troposphere (1).

During the last two decades, it has become clear that the appearance of tropospheric ozone is much less uniform than previously thought. Advances in measurement techniques have made it possible to demonstrate that tropospheric ozone variability can be resolved in a number of spatial and temporal scales. The variability is partly due to natural processes, but anthropogenic impact also perturbs the distribution and abundance of ozone.

It has become clear that ozone near the ground affects living systems in many important ways, and plays a very important role in numerous processes which affect the chemical composition of the troposphere.

Exposure to enhanced ozone concentrations may pose a risk to the public health. In the U.S. the ambient air quality standard for ozone is 120 ppbv as an hourly mean, not to be exceeded more than once per year. There are indications that exposure to slightly enhanced ozone concentrations (e.g. 60 ppbv) over a growing season, may cause significant yield reductions in many crops (2). Enhanced ozone concentrations also indicate increased photochemical activity, pointing to efficient production of sulphate and nitrate in air rich on nitrogen oxides and sulphur dioxide. Oxidation of SO_2 to sulphate in the liquid phase through reaction with dissolved ozone contributes significantly to the sulphate levels found in precipitation (3). The formation of the hydroxyl radical in clean air is determined by the reaction between excited state atomic oxygen and water vapour, and the concentration of excited state atomic oxygen is determined by the photodissociation of ozone for solar radiation of wavelength less than approx. 320 nm. Tropospheric ozone is very important for the infrared radiation budget of the atmosphere. The pressure broadening for ozone absorption causes the effective longwave optical depth of tropospheric ozone, which is proportional to pressure, to be nearly the same as that of stratospheric ozone (4). Fishman and colleagues (5) calculated that changes in tropospheric ozone due to anthropogenic activities at the end of the next century may have increased surface temperatures by nearly 1 K, which is a substantial number compared to the 2-3 K temperature increase calculated for a doubling of CO_2.

In this paper the distribution of ozone in different temporal and spatial regimes in the atmospheric boundary layer and the free troposphere is discussed. Measurements and model calculations are used to assess sources and sinks.

2 TEMPORAL AND SPATIAL REGIMES

2.1 Ozone in the atmospheric boundary layer

The atmospheric boundary layer (ABL), is under the direct influence of the ground through the exchange of heat, momentum, moisture and other gaseous and particulate material. The layer is mixed by convective activity during daytime over the continents when the ground is heated by solar radiation. The height of the mixed layer may extend up to 1-2 km during the summer, less during the winter. A typical time length between ABL break down situations is 2-4 d at mid latitudes (6). Break down may occur as a result of large-scale convective instability, at fronts through upsliding motion, in mountainous regions where the vertical mixing may be considerable, and by continuous synoptic-scale vertical motion in combination with the diurnal cycle of the depth of the boundary layer which causes the contents of the boundary layer to be pumped upwards in the middle of the day, where it is left behind to be acted upon by the steady synoptic upward motions.

Features of the ozone distribution which are characteristic for the ABL appear in a time range comparable to, or shorter than, the span between ABL break down situations. In Table 1 some characteristic phenomena have been outlined where enhanced ozone concentrations may be found.

Table 1: Spatial and temporal scales of some features of the ozone distribution in the atmospheric boundary layer.

Spatial scale	Temporal scale	Description
1-100 km	a few hours or less	Enhanced ozone concentrations in the plumes from refineries, petrochemical industry, power plants.
100 km	a few hours	Enhanced ozone concentrations in plumes from urban areas, forest fires.
1000 km	some days	Accumulation of ozone in air transported over long distances and in regional air masses in stagnant anticyclones.

Enhanced levels of ozone in the ABL are usually formed photochemically from emissions of hydrocarbons (HC), carbon monoxide (CO) and nitrogen oxides (NO and NO_2, the sum denoted NO_x). The rate determining step in the oxidation process is the initial reaction

$$HC + OH \rightarrow \text{aldehydes}, RO_2, HO_2 \qquad (R1)$$

where RO_2 and HO_2 are organic and inorganic peroxy radicals. If the hydrocarbons originate from some anthropogenic activity, they usually consist of light weight alkenes, alkanes or aromatic species. Alkenes may initially also react with ozone.

(R1) is followed by reactions where NO is converted to NO_2:

$$NO + RO_2 \rightarrow NO_2 + RO \qquad (R2)$$

$$NO + HO_2 \rightarrow NO_2 + OH \qquad (R3)$$

These reactions are fast and compete efficiently with other loss mechanisms for peroxy radicals in a moderately or strongly polluted ABL. NO_2 is photodissociated (M is a third body):

$$NO_2 + h\nu \rightarrow NO + O \qquad (R4)$$

and $$O + O_2 + M \rightarrow O_3 + M \qquad (R5)$$

Aldehydes formed through (R1) are photodissociated and peroxy radicals formed. Typically, the half life of the reactive hydrocarbons in moderately polluted air is a few hours, while the half life of slower reacting alkanes (methane not considered) may be a week or more.

Ozone may also be formed through reactions involving CO and NO_x:

$$CO + OH \xrightarrow{O_2} CO_2 + HO_2 \qquad (R6)$$

followed by (R3).
Initially, OH may be formed through the photodissociation of ozone

$$O_3 + h\nu \rightarrow O_2 + O(^1D) \qquad (R7)$$

for wavelengths below approx. 320 nm, followed by

$$O(^1D) + H_2O \rightarrow 2OH \qquad (R8)$$

The reaction rate coefficient for (R6) is only a few per cent (2.7×10^{-13} cm^3 (molecule $s)^{-1}$) of the reaction rate coefficients of OH with reactive hydrocarbons. Reaction (R6) is not a main contributor to ozone which is formed within the ABL, even though the concentraton of CO and the sum of nonmethane hydrocarbons may be comparable on a C-atom basis (of the order of 100 ppbC) in moderately polluted air. Only hydrocarbons which are reactive enough to decompose significantly during the time period between ABL break down situations, contribute much to ABL ozone formation.

There are numerous accounts of observations of ozone features listed in Table 1. In Norway, ozone plumes from a petrochemical factory which emits ethene, propene and other hydrocarbons, have been detected. The factory is at Rafnes in Southern Telemark (map see Figure 1), at a fjord where the

wind follows the land sea breeze pattern in the valley fjord system in fair weather during the summer. On two consecutive days during the summer of 1979, probably during accidentally high hydrocarbon emissions from the factories, nearly 200 ppbv as hourly maximum ozone concentration was observed in the sea breeze at Haukenes. The distance from the emissions was 12-15 km, and the wind speed was about 2 m/s, indicating a transport time of 2 h. The local build up was striking when comparing with the upwind ozone concentrations measured at the coastal station Langesund (Figure 1). A chemiluminescence technique was used to monitor ozone continuously (7).

High ozone concentrations in the smoke from a forest fire was observed in southern Telemark 26th and 27th August 1976 (Figure 2). On the 25th August 1976 there was a land sea breeze wind pattern (cpr. Figure 1) and the concentration of ozone peaked as the sea breeze front came in over the measurement site at Bjørnstadjordet in the morning hours, carrying a mixture of the emissions of the surrounding urban area and the the industrial emission from Herøya (NO_x, SO_2, Cl_2).
An extensive forest fire took place approx. 60 km north-northwest of Porsgrunn near Notodden (see Figure 1). At night 25th August the wind changed to a steady northnorthwest or northeast direction, both day and night (Figure 2). There was an impairment of the visibility due to smoke, and the smell was noticeable (8). At the same time the ozone concentration at the monitoring site in southern Telemark rose to more than 100 ppbv, and remained high for the next day or so. Trajectories calculated backwards 48 h, 850 mb, originated in the North Atlantic and did not cross pollution sources, It is likely that the excess ozone concentraton in the forest fire plume was several tens of ppbv. This is in agreement with findings made elsewhere (9, 10).

Power plant emission probably account for about one third of the NO_x emissions and half of the SO_2 emissions in western industrialized countries (11). During winter or in clean, stable air the chemical activity in a power plant plume is usually low. In fair weather situations with good atmospheric mixing, however, the formation of sulphate and nitrate may be significant in a power plant plume embedded in air moderately or heavily polluted with urban emissions.

If the concentration of ozone in the plume is higher than in the ambient air, the conditions are usually good for the oxidation of SO_2 and NO_x as well. Field studies in the U.S. have shown that ozone "bulges" in power plant plumes are fairly common 1-2 h downwind of the sources (12).

Model studies of the chemistry of power plant plumes in a moderately or strongly polluted ABL in fair weather, have shown that zones of enhanced photochemical activity first appear on the edges of the plume, later in the plume centre (13).

Substantial amounts of ozone may be generated in polluted air masses from an urban area. This has been seen most dramatically in the Los Angeles basin, where photochemcial air pollution has represented a serious threat to the public health during the last four decades. The pollutant transport from St. Louis has also been much studied. St. Louis is surrounded by fairly flat and unpolluted countryside in all directions.

Local sources do not affect the ageing air masses downwind of the city. White and coworkers (14) showed how secondary pollutants like ozone were formed, with concentration peaks 2-3 h downwind, see Figure 3. This has been simulated in a Lagrangian type urban plume model where a box volume passed over the St. Louis urban area, accumulated emissions of nitrogen

oxides, hydrocarbons and sulphur dioxide, and was then advected downwind (15). Each chemical constituent satisfied the continuity equation

$$\frac{dc}{dt} + \frac{1}{h}\frac{dh}{dt}(c-c_0) = P_c + P_e - (L_c + L_a + \frac{v_d}{h})\,c$$

where c was the concentration of the species calculated, h mixing height of the urban plume, c_0 concentration in ambient air, P_c and $L_c c$ chemical production and loss terms, P_e emissions, $L_a c$ aerosol adsorption, and $v_d c/h$ ground removal where v_d was the deposition velocity. In Figure 3 is shown the results of a St. Louis urban plume calculation for ozone, kept together with the measured development.

The next step in Table 1 is long-range transport. In Figure 4 is shown an example of flight measurements of long-range transported ozone coming in from the southeast over the coast of Southern Norway in the afternoon on July 9th, 1981 (16). The 96 h, 850 mb trajectory arriving at Birkenes at 18 GMT on July 9th, 1981 is also shown (17). Long-range transported ozone can be viewed as a "river" of enhanced ozone in the ABL. Ozone in plumes from cities, power plants, refineries or forest fires can also be seen as "rivers" of enhanced ozone in the ABL, each with characteristic dimensions in space and time.

A final feature of the distribution of the concentration of ozone in the ABL, is the diurnal variation seen e.g. in Figure 1. Over rural areas with low or non existent emissions of nitrogen oxides, ground removal causes the nocturnal decay in ozone close to the ground. Garland and Derwent (18) found that over a rural site covered with grass at Harwell in the U.K., the decay in the ozone concentration after sunset was nearly exponential on nice, sunny days. The exponential decay constants fell in the range 0.08 to 0.6 h^{-1}, corresponding to

lifetimes between 1 and 10 h. They found that the mean deposition velocity was 0.6 cm/s by day and 0.3 cm/s by night. Defining the reciprocal of the deposition velocity, usually called the resistance, as

$$r(z) = r_a(z) + r_b + r_s$$

where r_a is the resistance to transport in the turbulent boundary layer, r_b an additional resistance through the laminar layer next to the surface and r_s the resistance of the surface itself, they found that both the aerodynamic and surface components of the resistance increased at night. The behaviour of the surface resistance was not consistent with stomatal control, however. Galbally and Roy (19) found that the ozone up-take by vegetation was very dependent on stomatal resistance, and stomata are in general closed during the night resulting in a high value of r_s. In Figure 5 is shown the diurnal variation of the concentration of ozone at several heights in the nocturnal ABL at a rural site in New South Wales, Australia (20). Ground removal controlled the concentration of ozone. Bursts of turbulence gave rise to isolated peaks in ozone near the ground.

In anticyclonic weather when a low nocturnal inversion is established, ozone from the previous day may be trapped aloft. When convective elements erode the nocturnal inversion after sunrise, ozone rich air can be mixed down to the surface, at the same time as the photochemical activity may cause generation of ozone. The diurnal variation in the turbulent structure of the ABL in anticyclonic weather together with ground removal therefore give rise to the typical diurnal profile of the concentration of ozone.

The reaction

$$NO + O_3 \rightarrow NO_2 + O_2 \qquad (R9)$$

removes ozone at night. During daytime (R9) is followed by the photodissociation of NO_2 (R4) followed by (R5) causing no nett loss of ozone. During daytime, the peak in the ozone concentraton can be reinforced by the "smog" reactions (R1-R5).

2.2 Ozone in the free troposphere

The mixing time for a tracer released at the ground to reach the tropopause is 1-2 months as a global average. The exchange between the ABL and the free troposphere to a large extent takes place through the ascent in depressions, fronts, orographic systems, and penetrative convective systems like large cumulus and cumulonimbus clouds (6). The air which is drawn into young cumulus clouds originates close to the ground. Secondary products like ozone, or fresh emissions of hydrocarbons and nitrogen oxides can be transported by the vertical currents that feed these clouds from the ground level to altitudes well above the top of the mixed layer in one steady, upward motion. In the process, little or no mixing with aged pollutants in the mixed layer occurs. At night, cumulus clouds usually evaporate, leaving behind products of liquid phase reactions which can be transported over long distances by the nocturnal jet. The nocturnal jet is often established 300-500 m above the ground and appears when the stable layer next to the ground eliminates the transport of vertical momentum, hence the frictional drag on the horizontal flow disappears (21).

The exchange between the ABL and the free troposphere thus takes place through very efficient updrafts covering a limited area. Species of limited chemical lifetime, like ozone, nitrogen oxides and nonmethane hydrocarbons may penetrate through

the lower troposphere into the upper troposhere in vigorous, deep but infrequent cumulus transport. This is the only process rapid enough to move certain species into the upper troposphere before they are decomposed, and can give rise to in situ ozone production (22).

Table 2: Spatial and temporal scales of some features of the ozone distribution in the free troposphere.

Spatial scale	Temporal scale	Description
10 km	1 h	Cumulus cloud updrafts.
100 km	10 h	Stratospheric intrusion in tropopause folds (frontal zones).
100 km	Some h	Horizontal, shallow (a few hundred m thick) layers ("bands") of ozone rich air.

As indicated in Table 2, the temporal and spatial scales of typical features in the ozone concentration distribution in the free troposphere represent a complex picture. Ozone rich air of stratospheric origin may be exchanged with tropospheric air in a number of ways, discussed by Reiter (23) and summarized by Shapiro (24). Vertical mass exchange during tropopause folding events associated with extratropical cyclonic systems has been much studied, and can give rise to enhanced ozone concentrations all the way to the ground. From aircraft measurements, Danielsen and Mohnen (25) deduced that ozone transport took place during tropopause folding events by pointing to the positive correlation between the ozone mixing ratio and potential vorticity and between potential vorticity and ^{90}Sr radioactivity. Potential vorticity is defined as

$$P_\theta = - (\zeta_\theta + f) \frac{\delta\theta}{\delta p}$$

where $\zeta_\theta = \frac{\delta v}{\delta x} - \frac{\delta u}{\delta y}$, u and v are the zonal and meridional components of the wind, f the vertical component of the

earth's vorticity, ζ_θ is the relative vorticity on an isentropic surface $\delta\theta/\delta p$ the thermal stability. The tropopause appears as a zero-order discontinuity in P_θ, with a one to two orders of magnitude drop in its value passing into the troposphere (24). ^{90}Sr is an Sr-isotope which is a unique tracer of nuclear bomb debris, and consequently of stratospheric air.

Danielsen and Mohnen (25) concluded that ozone-rich air is transported into the troposphere with each major cyclonic development. Ozone-rich air can occasionally reach the ground with concentrations exceeding air quality standards. The appearance at the ground was strongly asymmetrical due to the narrowness of the folded structure and the deformation of the descending air. Some local regions were influenced by the ozone-rich layers for 2-3 h, others for 1-2 d, cpr. Table 2.

Derwent and coworkers (26) reported two springtime occurrences at a rural site in the U.K. of elevated ozone concentration, 100 ppbv, over periods of 1-3 d in circumstances when ABL photochemical generation could be disregarded (in March 1974 at Harwell, Oxfordshire and in March 1977 at Sibton in Suffolk). The temperatures were low, with high cloud cover, moderate wind and absence of nocturnal inversions. The synoptic situations were characteristic for the types giving rise to intrusions of stratospheric air. Furthermore, the high concentrations of ozone were observed at a single site only each time. Simultaneous measurements of an anthropogenic tracer, F-11, showed concentrations typical of clean Northern Hemispheric background air, the sulphate levels were low, and measurements of radon (which is emitted continuously from the ground) showed low values with little evidence of nocturnal accumulation typical of increased atmospheric stability. The low concentrations of radon were taken as indication that the vertical mixing was efficient, with a significant source of ozone aloft necessary to account for the high ground level concentrations. Even more chemical evidence was collected: the episodes occurred roughly at the same time as the maximum total ozone during 1974 and 1977 near the measuring sites was observed, and they probably also coincided with the measured

annual peak in ground level air concentrations of radioactive debris from the stratosphere.

Shapiro (24) reported a case study of a tropopause folding event over the western part of the U.S., where aircraft was used to measure meteorological and chemical parameters (condensation nuclei and ozone). In Figure 6 is shown the ozone concentration analysis in the tropopause fold. The condensation nuclei count (typical concentrations were 10^3-10^4 particles/cm^3 in the ABL, 10^2 particles/cm^2 or less in the stratosphere) showed that the tropopause fold contained concentrations of condensation nuclei comparable to what is found in the ABL. Shapiro concluded that the tropopause folds are mixing regions with chemical characteristics somewhere between those of the troposphere and the stratosphere. Analysis of traces of ozone, condensation nuclei count and potential temperature through the lower part of the tropopause fold showed that the 10 km wavelength perturbations of the traces were the primary contributors to the turbulent fluxes within the fold. Turbulent mixing was found to be of first-order importance as a mechanism for stratospheric-tropospheric chemical exchange in the vicinity of tropopause folds.

Turbulent entrainment within tropopause folds takes place almost exclusively within the latitude belt most dominated by anthropogenic sources of chemicals. The time between release and stratospheric injection is of the order of a few h, with little time for tropospheric photochemical or precipitation processes to modify and reduce the effect on the stratosphere. It is not known how important this exchange mechanism is compared to others, e.g. the Hadley circulation in the subtropics where typically several weeks may pass for an air parcel to migrate from its chemical source region, into the Hadley circulation and into the stratosphere, allowing tropospheric chemical processes sufficient time to modify the composition of the air parcel (24).

A third feature of the distribution of ozone in the free troposphere is mentioned in Table 2. "Bands" of ozone-rich air have been discovered using fast response ozone instruments in aircraft. In the GAMETAG experiment, mostly horizontal but also some vertical transepts, were taken in the free troposhere over the Pacific Ocean from Alaska southwards to New Zealand at 60^0S in 1977 and 1978. Significant layering was found, and it was said that "from the horizontal and vertical O_3 gradients observed, one is led to the tentative conclusion that a three-dimensional projection of a given O_3 layer is likely to define a shallow river in its geometric configuration" (27). Also found was a significant anti-correlation between the concentration of ozone and the dew point temperature (27).

Fishman and coworkers (28, 29) published the results of aircraft measurements of the simultaneous vertical distribution of CO and O_3 over the North Atlantic as far north as 67^0N and along the west coast of the American continent as far south as 57^0S. A significant layering of ozone was found to be present, but almost exclusively in the Northern Hemisphere. Elevated concentrations of O_3 and CO were often found concurrently, see Figure 7. It has been speculated that a significant in situ source of tropospheric ozone exists, cpr. reaction R7 followed by R8, R6, R3 and R4 (30).

2.3 Tropospheric ozone budget

The concentraton distribution of ozone in the troposphere has been shown to be nonuniform, both in time and space. The variation uncovered both in the ABL and the free troposphere, gives information about the production and loss mechanisms for ozone. The global, or climatological role of ozone in the troposphere can be investigated by looking at the distribution of ozone averaged over a time period of interest for global transport, e.g. one month. Averaged over one month there are

important variations in the tropospheric ozone distribution. In Figure 8 is shown the monthly average ozone concentration for three ozonesonde stations, at the 200 and 800 mb level (30). At 200 mb, a distinct annual maximum was present in the late winter and early spring. The amplitude of the annual cycle and the absolute concentrations of all three data sets were very similar, as a result of downward transport from the stratosphere combined with the fact that the average tropopause height was lower during that part of the year. The 800 mb data sets were less similar. The seasonal variation was very marked in the Northern Hemisphere and virtually nonexistent at Aspendale. Also the Southern Hemisphere concentration at Aspendale was much less than what was measured at Northern Hemisphere mid-latitudes. The hemispheric difference has also been demonstrated by aircraft measurements, see Figure 8, the lower part. A minimum was found near 10^0 S in all profiles.

The tropospheric ozone budget can be divided into four components, each of comparable magnitude: transport from the stratosphere, destruction at the ground, photochemical production and photochemical destruction. Fishman (31) reviewed the estimates available from measurements and model calculations of the components of the tropospheric ozone budget, and summarized the results as shown in Table 3.

Table 3: Tropospheric ozone budget (31).

	Northern Hemisphere	Southern Hemisphere	References
	(in 10^{11} molecules $cm^{-2} s^{-1}$)		
Transport from the stratosphere	0.5-0.8	0.3-0.4	25, 32, 33
Destruction at the ground	0.7-1.4	0.4-0.8	19, 33
Photochemical destruction	1.9-2.2	1.1-1.2	30, 34-36
Photochemical production	1.9-3.1	1.1-2.9	30, 34-36

Danielsen and Mohnen (25) estimated the stratospheric flux through simultaneous aircraft measurements of ^{90}Sr and ozone. Mahlman et al. (32) applied the Princeton General Fluid Dynamics Laboratory (GFDL) general circulation model (37) to calculate the transport of ozone through the tropopause. Gidel and Shapiro (33) combined calculations of potential vorticity fluxes with observed ozone distributions to estimate average nett vertical fluxes of ozone of .49 and .25 x 10^{11} molecules cm^{-2} s^{-1} for the Northern and Southern Hemispheres, respectively. There is a high correlation between zonal means of ozone and potential vorticity. Gidel and Shapiro (33) also estimated the surface deposition fluxes for ozone, and found 0.82 and 0.48 x 10^{11} molecules cm^{-2} s^{-1} for the Northern and Southern Hemispheres, respectively. They concluded that there seemed to be a hemispherically asymmetric photochemical source of ozone in the troposphere. Fishman (31) reevaluated the deposition estimates by Galbally and Roy (19) on the basis of improved knowledge of ozone concentration distributions, surface type and ozone deposition velocities, and found a Southern Hemispheric average deposition flux of 5.6 x 10^{10} molecules cm^{-2} s^{-1}, 16.9 x 10^{10} in the Northern Hemisphere. The large difference reflected both the greater abundance of ozone in the Northern Hemisphere and the greater amount of landmass where the ozone ground removal is efficient.

Fishman (31) concluded on the basis of the investigations summed up in Table 3, that mechanisms in addition to stratospheric injection and surface removal of $11 \pm 8 \times 10^{10}$ molecules cm^{-2} s^{-1} were needed to balance the tropospheric ozone budget in the Northern Hemisphere, $3 \pm 5 \times 10^{10}$ molecules cm^{-2} s^{-1} in the Southern Hemisphere. Photochemical destruction of tropospheric ozone mainly takes place through the reaction (R7) followed by (R8), and through

$$O_3 + OH \rightarrow HO_2 + O_2 \qquad (R10)$$

followed by

$$O_3 + HO_2 \rightarrow OH + 2O_2 \qquad (R11)$$

Fishman et al. (30) estimated that integrated through the Northern Hemisphere using a photochemical model for tropospheric ozone, reaction (R8) accounted for 52% of the photochemical loss of tropospheric ozone, (R11) 42% and (R10) 6%. In Table 3 it is shown that on the basis of several investigations, a photochemical loss rate of $21 \pm 4 \times 10^{10}$ molecules cm^{-2} s^{-1} is calculated for the Northern Hemisphere, $11 \pm 3 \times 10^{10}$ for the Southern Hemisphere.

The calculation of the photochemical production rate of ozone in the troposhere is more controversial than the calculation of the photochemical destruction rate, which relies mostly on the data for the ozone concentration distribution and the a photolysis at short wavelengths. To estimate the production of ozone, however, the NO_x concentration distribution must be known. This point is clearly seen from Figure 9, where model-derived, annual mean photochemical production and destruction rates of tropospheric ozone in the Northern Hemisphere as a function of the prescribed NO_x concentrations, are shown (30). It can be seen that at approx. 25 pptv of average NO_x, there is a balance between production and destruction, a somewhat higher average NO_x concentration would be required to balance the tropospheric ozone budget (Table 3).

Figure 9 can be understood as follows:

The predominant production of ozone takes place through reaction R2 or R3 followed by R4 and R5. The HO_2 radical is recycled from OH mainly through R6. Methane is a principal source of OH and HO_2 radicals. Other natural and anthropogenic hydrocarbons contribute. The HO_2 radical is involved in both production (R3) and loss processes of ozone (R11), and the concentration ratio of O_3 to NO is therefore critical for the nett effect. At low NO concentrations, HO_2 radicals may also be efficiently lost through

$$HO_2 + HO_2 \rightarrow H_2O_2 + O_2 \qquad (R12)$$

$$HO_2 + CH_3O_2 \rightarrow CH_3O_2H + O_2 \qquad (13)$$

where the products may be photolysed, react with hydroxyl or dissolved in water droplets.

The concentration distribution of NO and NO_2 in the troposphere is highly variable. Concentrations as low as a few pptv of NO have been measured for noontime conditions e.g. in the equatorial Pacific region (38). NO_x concentrations of 13 ppv (NO 4 pptv) have been measured during daylight at a remote site in the Colorado mountains (38). In a moderately polluted ABL, NO_x is typically a few ppbv. Over urban areas, the NO_x concentrations typically may reach several hundred ppbv during daytime, with NO as the dominating species (40). The concconcentration of NO and NO_2 in the troposphere may therefore span more than three orders of magnitude, and it is not meaningful to define a representative distribution of tropospheric NO_x. An attempt at a source inventory of tropospheric NO_x is shown in Table 4. The anthropogenic source is the dominating one. It should be remembered, however, that NO_x injected into the troposphere from the stratosphere is less affected by rainout and has a much longer lifetime than ground level NO_x.

Table 4: Sources of tropospheric NO_x, in TgN/y. ($T=10^{12}$) (41).

	TgN/y	Comments
Anthropogenic ground level sources	20	Mainly at mid latitudes, Northern Hemisphere.
Lightning	3.5	
Downward flux from the stratosphere	.3	Results from the stratospheric reaction $N_2O + O(^1D) \rightarrow 2NO$.
High flying aircraft	.5	

This means that NO_x of stratospheric origin can participate longer in the ozone production before it is removed, than what is the case for low level emissions of NO_x (41).

Due to the uneven distribution of NO_x, the photochemical production of tropospheric ozone is also highly variable with time and in space, with regions where the NO_x deficiency causes a nett photochemical destruction of ozone, and other regions with a significant nett production. The positive correlation of the short term fluctuations of the concentrations of ozone and carbon monoxide as measured by Fishman and Seiler (28, 29, 42) in the free troposphere between 15^0N and 45^0N led to the conclusion that there is a photochemical source of ozone in this region. The low levels of NO_x in the equatorial Pacific region indicate a nett ozone sink there. This is supported by the meridional distribution of the concentration of ozone, which decreases towards the Intertropical Convergence Zone (43, 44).

Calculations with a 2-dimensional, meridional model of the photochemistry and zonally averaged transport of the tropo - sphere, showed that approx. 50% higher ozone concentrations were obtained for the lower troposphere at the polluted mid-latitudes in the Northern Hemisphere than in the Southern Hemisphere. Outside the regions influenced by pollutant sources, the low levels calculated for the concentration of NO did not favour photochemical production of ozone (45). Similar calculations by Crutzen and Gidel (41) showed that the best agreement with the global observations of ozone was obtained if industrial sources of NO_x and hydrocarbons were included.

3 TROPOSPHERIC OZONE AND CLIMATE

Observations of the distribution of the concentration of ozone in the atmospheric boundary layer and the free troposphere have revealed a large degree of variability (within an order of magnitude) over a few hours' time, some tens or hundreds of kilometers horizontally and a few hundred meters vertically. Although the observational support was sparse, the variability seemed to prevail largely in the Northern Hemisphere. Averaged over some period of time, e.g. one month, the observations of tropospheric ozone indicated that there was a spring maximum at all altitudes in the troposphere, and there was a maximum in the meridional distribution around 35^0N. Model calculations have indicated that the Northern Hemisphere excess ozone was caused by anthropogenic activity, chiefly emissions of CO, NO_x and hydrocarbons from the burning of fossile fuels.

Fishman and coworkers (5) argued on the basis of calculations with a radiative transfer model (4) that the Northern Hemisphere could be warmer than the Southern Hemisphere by about 0.2 K because of the larger amount of ozone in the Northern Hemisphere.

Model calculations of the future composition of the atmophere have indicated that a significant increase in tropospheric ozone may take place if the emissions of CO, NO_x and HC are increasing steadily. (A doubling by the end of the next century, 46). On the basis of these projections, it has been calculated that the global surface temperature may increase by 0.9 K if the tropospheric ozone concentrations were doubled (5). Angell and Korshover (47) have shown on the basis of ozone sonde measurements at 2-8 km altitude that there has been a 20% increase in the ozone concentrations at mid latitudes in the Northern Hemisiphere from 1970-1980. Measurements in polar regions have shown a similar increase, which excludes the possibility of a limited smog effect only.

The number 0.9 K should be compared with the calculated effect on the surface temperature of the increase in the atmospheric burden of several other trace gases which are infrared absorbers.

Lacis et al. (48) calculated the change in the surface equilibrium temperature (the greenhouse effect) for several trace gases which increase in abundance in the atmosphere, see Table 4.

Table 5: Greenhouse effects (ΔT_{eq} in K) of methane, nitrous oxide, chlorofluorocarbons (F-11 and F-12) and carbon dioxide (48).

Species	Concentration Initial	Final	ΔT_{eq}	1970-1980 change in concentration 1970	1980	ΔT_{eq}
CH_4 (ppmv)	1.6	3.2	0.26	1.5	1.65	.032
N_2O(ppbv)	280	560	0.65	295	301	.016
CCl_3F(ppbv)	0	2	0.29	.045	.135	.020
CCl_2F_2 (ppbv)	0	2	0.36	.125	.315	.034
CO_2 (ppmv)	300	600	2.9	325	337	0.14

These calculations were based on the assumption that the scenarios were equilibrium situations. If the atmospheric infrared absorption is changed for some period of time which is short compared to the time required for the planet to approach a new equilibrium temperature (a few years, 49), the global warming would be much less than the warming at equilibrium. The climatic impact of changes in tropospheric ozone on a time scale of the order of one year or less, would therefore be small. Long term changes can be climatologically very significant, however.

ACKNOWLEDGEMENT

Dr. Jack Fishman at NASA Langley Research Center, Hampton, VA has contributed significantly to this paper through the communication of a preprint of ref. 31.

REFERENCES AND NOTES

(1) Junge, C.E. (1962) Global ozone budget and exchange between stratosphere and troposphere. Tellus 14, 363-377.

(2) Heck, W.W., O.C. Taylor, R. Adams, G. Bingham, J. Miller, E. Preston and L. Weinstein (1982) Assessment of crop loss from ozone. JAPCA 32, 353-361.

(3) Penkett, S.A., B.M.R. Jones, K.A. Brice and A.E.J. Eggleton (1979) The importance of atmospheric ozone and hydrogenperoxide in oxidising sulphur dioxide in cloud and rainwater. Atmospheric Environment 13, 123-127.

(4) Ramanathan, V. and R.E. Dickinson (1979) The role of stratospheric ozone in the zonal and seasonal radiative energy balance of the earth-troposphere system. J.Atm.Sci. 36, 1084-1104.

(5) Fishman, J., V. Ramanathan, P.J. Crutzen and S.C. Liu (1979) Tropospheric ozone and climate. Nature 282, 818-820.

(6) Smith, F.B. and D.J. Carson (1977) Some thoughts on the specification of the boundary layer relevant to numerical modelling. Boundary Layer Met. 12, 307-330.

(7) Schjoldager, J. and L. Stige (1980) Measurements of ozone in Southern Telemark, Oslo and the Oslo fjord during the summer 1979. NILU OR 5/80. Box 130, N-2001 Lillestrøm, Norway, 56 p (in Norwegian).

(8) Schjoldager, J., B. Sivertsen and J.E. Hanssen (1978) On the occurrence of photochemical oxidants at high latitudes. Atmospheric Environment 12, 2461-2467.

(9) Evans, L.F., I.A. Weeks, A.J. Eccleston and D.R. Packham (1977) Photochemical ozone in smoke from prescribed burning of forests. Environ. Sci. Technol. 11, 896-900.

(10) Stith, J.L., L.F. Radke and P.V. Hobbs (1981) Particle emissions and the production of ozone and nitrogen oxides from the burning of forest slash. Atmospheric Environment 15, 73-82.

(11) Semb, A. (1979) Emission of gaseous and particulate matter in relation to long-range transport of air pollutants. Proceedings, WMO symposium, Sofia 1-5 October 1979, WMO No. 538, Geneva, pp. 1a-1m.

(12) Davis, D.D., G. Smith and G. Klauber (1974) Trace gas analysis of power plant plumes via aircraft measurements. O_3, NO_x and SO_2 chemistry. Science 186, 733-736.

(13) Hov, Ø. and I.S.A. Isaksen (1981) Generation of secondary pollutants in a power plant plume: A model study, Atmospheric Environment 15, 2367-2376.

(14) White, W.H., J.A. Anderson, D.L. Blumenthal, R.B. Husar, N.V. Gillani and J.D. Husar (1976) Formation and transport of secondary air pollutants: ozone and aerosols in the St.Louis urban plume. Science 194, 187-189.

(15) Isaksen, I.S.A., E. Hesstvedt and Ø. Hov (1978) A chemical model for urban plumes: Test for ozone and particulate sulfur formation in St. Louis urban plume. Atmospheric Environment 12, 599-604.

(16) Svelle, M. (Ed.) (1982) National program for the monitoring of pollution. Annual report 1981. The Norwegian State Pollution Control Authority, Oslo, Report 65/82, p. 35 (in Norwegian).

(17) The trajectories were calculated by Jørgen Saltbones at the Norwegian Meteorological Institute, Oslo.

(18) Garland, J.A. and R.G. Derwent (1979) Destruction at the ground and the diurnal cycle of concentration of ozone and other gases. Quart.J. Royal Meteorol. Soc. 105, 169-183.

(19) Galbally, I.E. and C.R. Roy (1980) Destruction of ozone at the earth's surface. Quart.J.Royal Meteorol. Soc. 106, 599-620.

(20) Galbally, I.E. (1967) Some measurements of ozone variation and destruction in the atmospheric surface layer. Nature 218, 456-457.

(21) Lamb, R.G. (1981) A regional scale model (1000 km) of photochemical air pollution, part I: Model formulation. EPA draft report, U.S. EPA, Research Triangle Park, North Carolina.

(22) Gidel, L.T. (1983) Cumulus cloud transport of transient tracers. J. Geophys. Res. 88, 6587-6599.

(23) Reiter, E.R. (1975) Stratospheric-tropospheric exchange processes. Rev.Geophys.Space Phys. 13, 459-474.

(24) Shapiro, M.A. (1980) Turbulent mixing within tropopause folds as a mechanism for the exchange of chemical constituents between the stratosphere and troposphere. J.Atm.Sci. 37, 994-1004.

(25) Danielsen, E.F. and V.A. Mohnen (1977) Project Duststorm report: Ozone transport, in situ measurements, and meteorological analyses of tropopause folding. J.Geophys.Res. 82, 5867-5877.

(26) Derwent, R.G., A.E.J. Eggleton, M.L. Williams and C.A. Bell (1978) Elevated ozone levels from natural sources. Atmospheric Environment 12, 2173-2177.

(27) Routhier, F., R. Dennett, D.D. Davis, A. Wartburg, P. Haagenson and A.C. Delany (1980) Free tropospheric and boundary-layer airborne measurements of ozone over the latitude range of 58^{0}S to 70^{0}N. J.Geophys.Res. 85, 7307-7321.

(28) Fishman, J., W. Seiler and P. Haagenson (1980) Simultaneous presence of O_3 and CO bands in the troposphere. Tellus 32, 456-463.

(29) Seiler, W. and J. Fishman (1981) The distribution of carbon monoxide and ozone in the free troposphere. J.Geophys.Res. 86, 7255-7265.

(30) Fishman, J., S. Salomon and R.J. Crutzen (1979) Observational and theoretical evidence in support of a significant in-situ photochemical source of tropospheric ozone. Tellus 31, 432-446.

(31) Fishman, J. (1983) Ozone in the troposphere. Unpublished manuscript. NASA Langley Research Center, Hampton, VA.

(32) Mahlman, J.D., H. Levy II and W.J. Moxim (1980) Three-dimensional tracer structure and behavior as simulated in two ozone precursor experiments. J.Atmos.Sci. 37, 655-685.

(33) Gidel, L.T. and M.A. Shapiro (1980) General circulation estimates of the net vertical flux of ozone in the lower stratosphere and the implications for the tropospheric ozone budget. J.Geophys.Res. 85, 4049-4058.

(34) Liu, S.C., D. Kley, M.McFarland, J.D. Mahlman and H. Levy II (1980) On the origin of tropospheric ozone. J.Geophys.Res. 85, 7546-7552.

(35) Logan, J.A., M.J.Prather, S.C. Wofsy and M.B.McElroy (1981) Tropospheric chemistry: A global perspective. J.Geophys.Res. 86, 7210-7254.

(36) Chameides, W.L. and A. Tan (1981) The two-dimensional diagnostic model for OH: an uncertainty analysis. J.Geophys.Res. 86, 5209-5224.

(37) Mahlman, J.D. and W.J. Moxim (1978) Tracer simulation using a global general circulation model: Results from a midlatitude instantaneous source experiment. J.Atmos. Sci. 35, 1340-1374.

(38) McFarland, M., D. Kley, J.W. Drummond, A.L. Schmeltekopf and R.H. Winkler (1979) Nitric oxide measurements in the equatorial Pacific region. Geophys.Res.Lett. 6, 605-608.

(39) Bollinger, M.J., D.D. Parrish, C. Hahn, D.L. Albritton and F.C. Fehsenfeld (1982) NO_x measurements in clean continental air. Proc. 2nd symposium: Composition of the nonurban troposphere, American Met.Soc., Boston, pp. 6-8.

(40) Hov, Ø. and S. Larssen (1984) Street canyon concentrations of nitrogen dioxide in Oslo. Measurements and model calculations. Env.Sci.Technol. (in the press).

(41) Crutzen, P.J. and L.T. Gidel (1983) A two-dimensional photochemical model of the atmosphere. 2: The tropospheric budgets of the anthropogenic chlorocarbons, CO, CH_4, CH_3Cl and the effect of various NO_x sources on tropospheric ozone. J.Geophys.Res. 88, 6641-6661.

(42) Fishman,J. and W. Seiler (1982) The correlative nature of ozone and carbon monoxide in the troposphere: implications for the tropospheric ozone budget. J.Geophys.Res. (submitted).

(43) Liu, S.C., M.McFarland, D. Kley, D. Zafiriou and B. Huebert (1983) Tropospheric NO_x and O_3 budgets in the equatorial Pacific. J.Geophys.Res. 88, 1360-1368.

(44) Davis, D.D., W.L. Chameides and C.S. Kiang (1982) Measuring atmospheric gases and aerosols. Nature 295, 186.

(45) Isaksen, I.S.A. (1979) Transport and distribution of pollutants in the troposphere. Proc. WMO Symp. WMO No. 538, Geneva, pp. 347-358.

(46) Logan, J.A., M.J. Prather, S.C. Wofsy and M.B. McElroy (1978) Atmospheric chemistry: Response to human influence. Trans.Roy.Soc. London 290, 187-234.

(47) Angell, J.K. and Korshover, J. (1980) Update of ozone variations through 1979. Proc. Quadrenniel international ozone symposium, Boulder, CO. 4-9 August 1980, ed. J. London, pp. 393-396.

(48) Lacis, A., J. Hansen, P. Lee, T. Mitchell and S. Lebedoff (1981) Greenhouse effect of trace gases, 1970-1980. Geophys.Res.Lett. 8, 1035-1038.

(49) Hansen, J., D. Johnson, A. Lacis, S. Lebedoff, P. Lee, D. Rind and G. Russel (1981) Climate impact of increasing carbon dioxide. Science 213, 957-966.

Figure legends

Figure 1: Hourly average ozone concentrations measured at Haukenes on June 5-8, 1979, 15 km downwind of the petrochemical industry at Rafnes. Upwind ozone concentrations measured at the coastal site at Langesund are shown for comparison (7).

Figure 2: Hourly average ozone concentrations measured at Bjørnstadjordet in Porsgrunn during a period with an extensive forest fire west of Notodden (see map, Figure 1). The forest fire smoke was clearly visible and the odour could be felt. The local wind speed and direction measured at Lakollen (Figure 1) is also indicated (9).

Figure 3: Observed and calculated ozone concentrations in the urban plume from St.Louis. Primary pollutants from St.Louis were emitted between 0600 and 0900 h in the model calculation. The calculated development of the concentration of ozone outside the urban plume is also shown (14,15).

Figure 4: Measured concentrations of ozone from aircraft on July 9, 1981, around 1600 h, along the coast between Arendal and Mandal. The flight level was 100-200 m. The 96 h, 850 mb back trajectory to Birkenes at 1800 GMT is also shown (17). Compare the map, Figure 1. (16).

Figure 5: The nocturnal variation of the concentration of ozone with time measured at heights indicated on the curves at a rural site in New South Wales, Australia. The inversion height was approx. 140 m (20).

Figure 6: Ozone concentrations in pphmv measured from two flight missions across a tropopause folding event at 00 GMT 13 March 1978. The troposphere is the stippled area. Two flight tracks are indicated, the ozone analysis for the upper flight track is dotted, for the lower flight track solid lines (24).

Figure 7: Vertical profiles of the concentration of O_3 and CO measured from an aircraft descent over Frobisher Bay, Northeast Canada (64^0 N) 25 July, 1974. Arrows indicate significant altitudes where anomalously high/low O_3 and CO concentration were found (28).

Figure 8: (Upper part) Monthly variation of the concentration of ozone at 200 mb and 800 mb at Boulder (40^0 N), the combined data from Bedford (42^0 N) and Wallops Island (38^0 N) and from Aspendale (48^0 S) (30).
(Lower part) Measured latitudinal distribution of ozone as compiled by Seiler and Fishman (29). Open quadrates denote the tropospheric average obtained in the flights described in (29), open triangles 480 mb, outbound leg, open circles 480 mb, homebound leg (29), crosses ref. (27).

Figure 9: Calculated Northern Hemispheric average, annual mean production and destruction rates of tropospheric ozone as a function of average NO_x concentration (30).

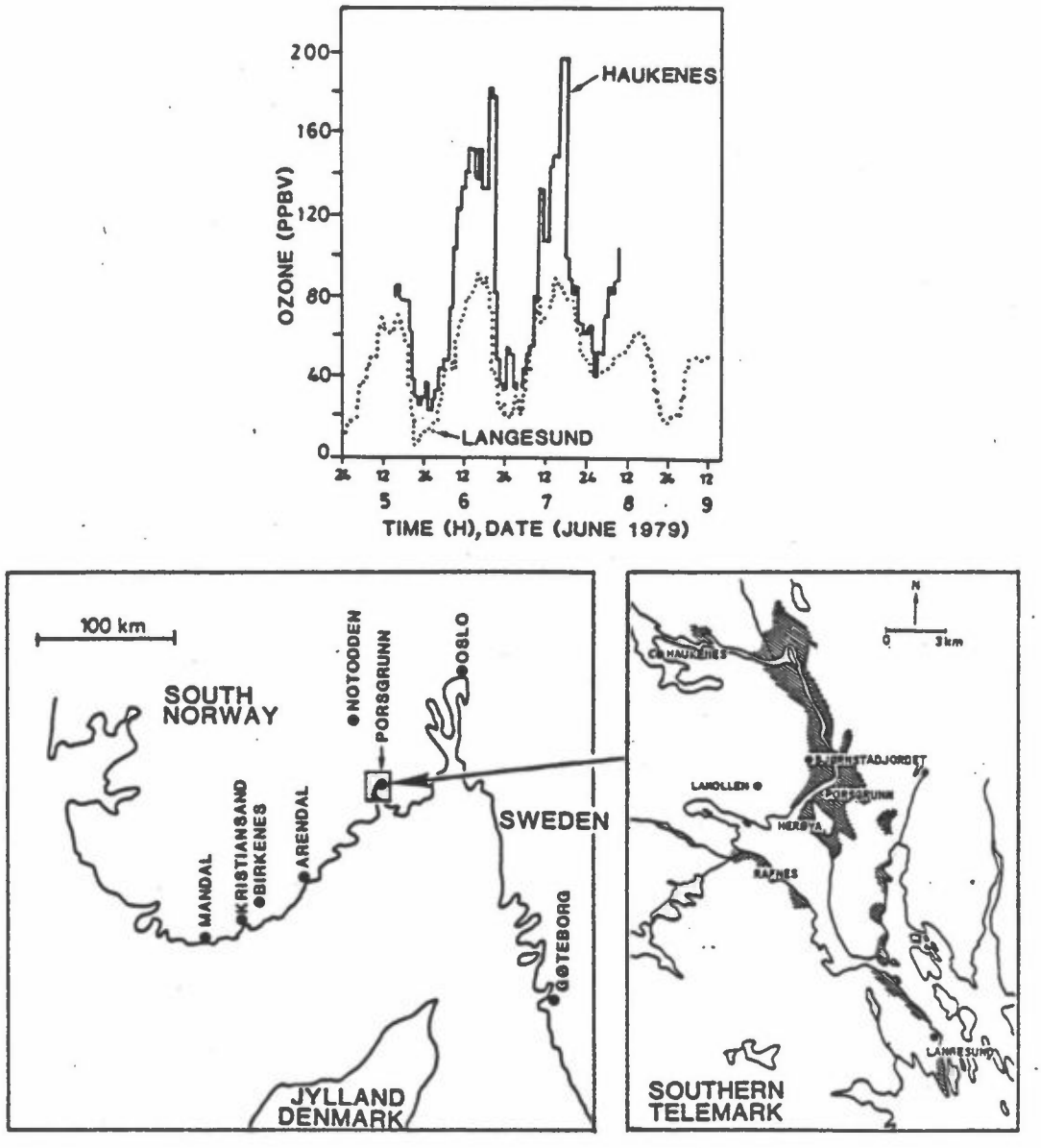

Figure 1: Hourly average ozone concentrations measured at Haukenes on June 5-8, 1979, 15 km downwind of the petrochemical industry at Rafnes. Upwind ozone concentrations measured at the coastal site at Langesund are shown for comparison (7).

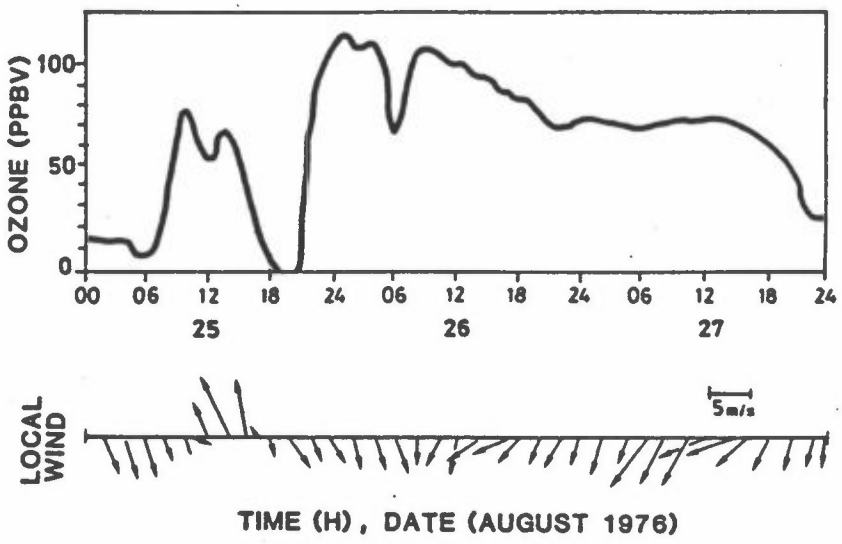

Figure 2: Hourly average ozone concentrations measured at Bjørnstad-jordet in Porsgrunn during a period with an extensive forest fire west of Notodden (see map, Figure 1). The forest fire smoke was clearly visible and the odour could be felt. The local wind speed and direction measured at Lakollen (Figure 1) is also indicated (9).

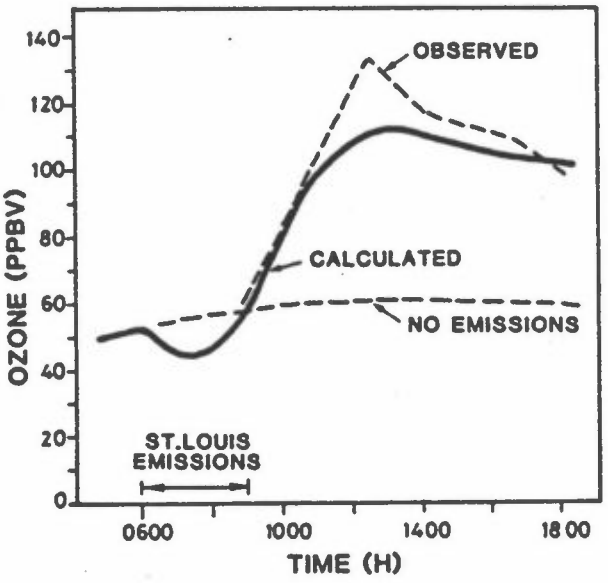

Figure 3: Observed and calculated ozone concentrations in the urban plume from St.Louis. Primary pollutants from St.Louis were emitted between 0600 and 0900 h in the model calculation. The calculated development of the concentration of ozone outside the urban plume is also shown (14,15).

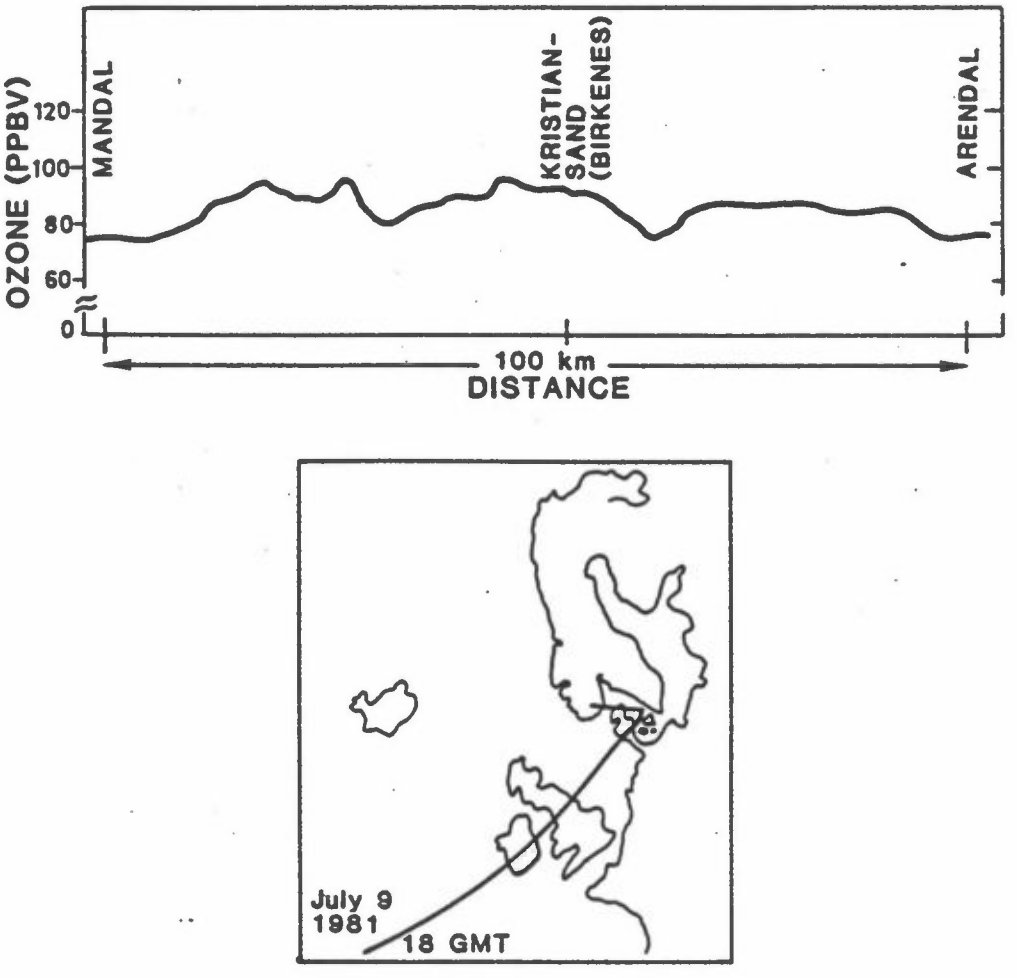

Figure 4: Measured concentrations of ozone from aircraft on July 9, 1981, around 1600 h, along the coast between Arendal and Mandal. The flight level was 100-200 m. The 96 h, 850 mb back trajectory to Birkenes at 1800 GMT is also shown (17). Compare the map, Figure 1. (16).

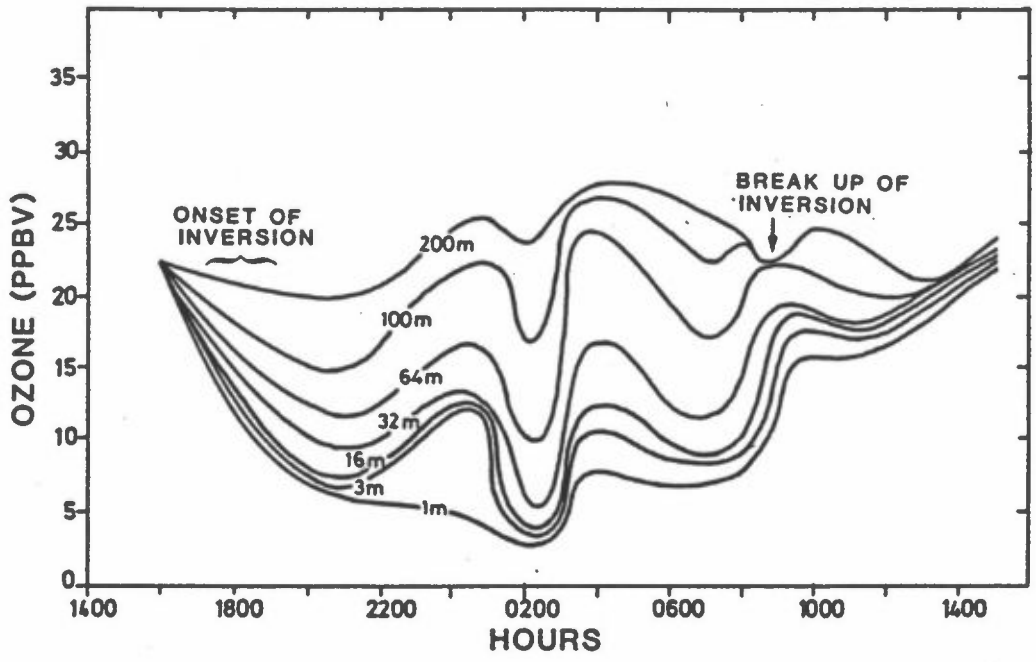

Figure 5: The nocturnal variation of the concentration of ozone with time measured at heights indicated on the curves at a rural site in New South Wales, Australia. The inversion height was approx. 140 m (20).

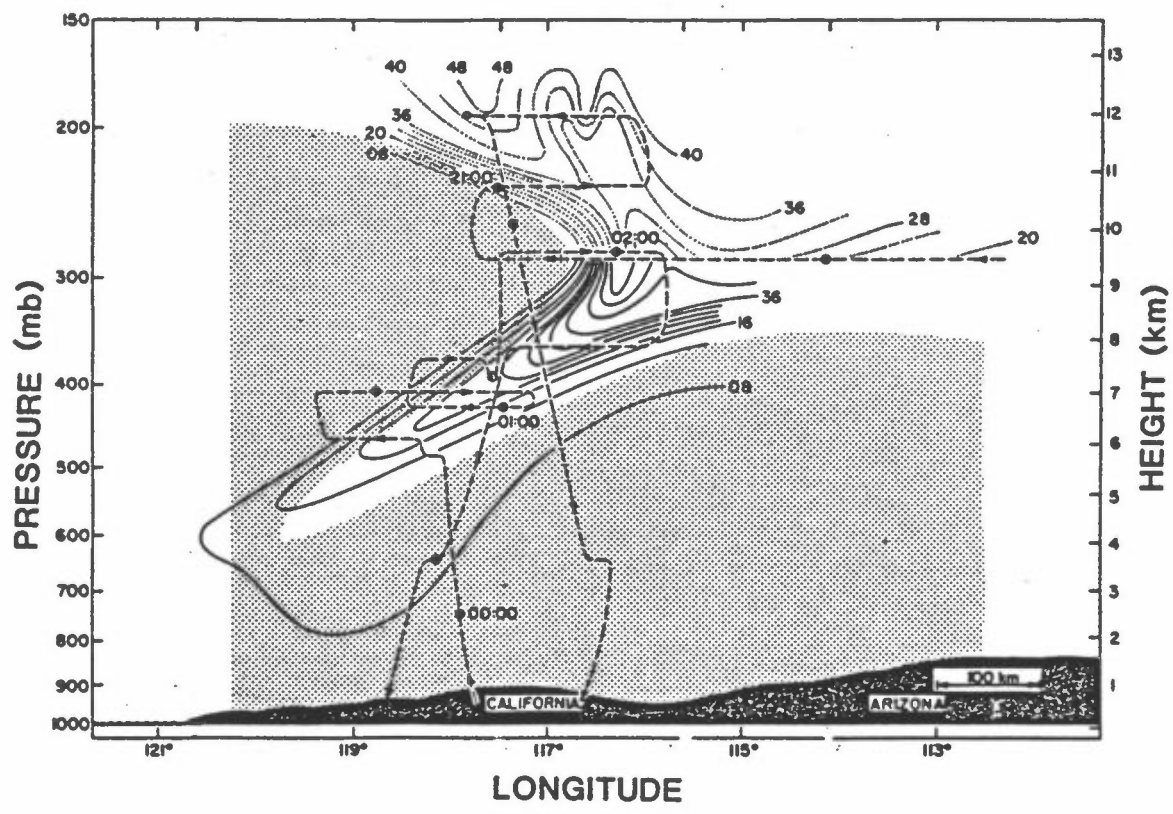

Figure 6: Ozone concentrations in pphmv measured from two flight missions across a tropopause folding event at 00 GMT 13 March 1978. The troposphere is the stippled area. Two flight tracks are indicated, the ozone analysis for the upper flight track is dotted, for the lower flight track solid lines (24).

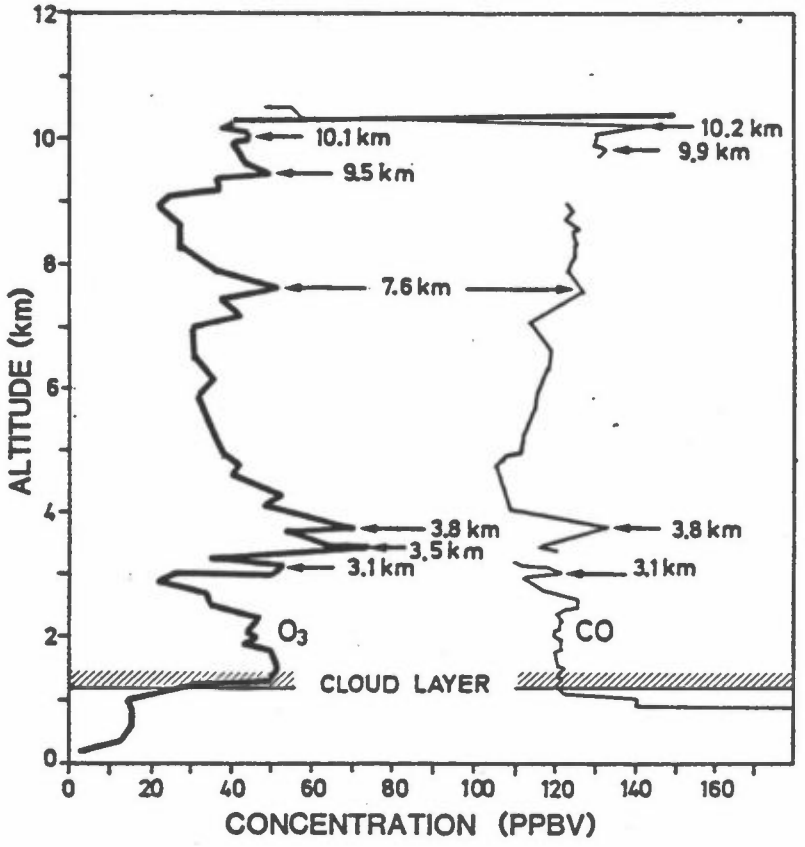

Figure 7: Vertical profiles of the concentration of O_3 and CO measured from an aircraft descent over Frobisher Bay, Northeast Canada (64° N) 25 July, 1974. Arrows indicate significant altitudes where anomalously high/low O_3 and CO concentration were found (28).

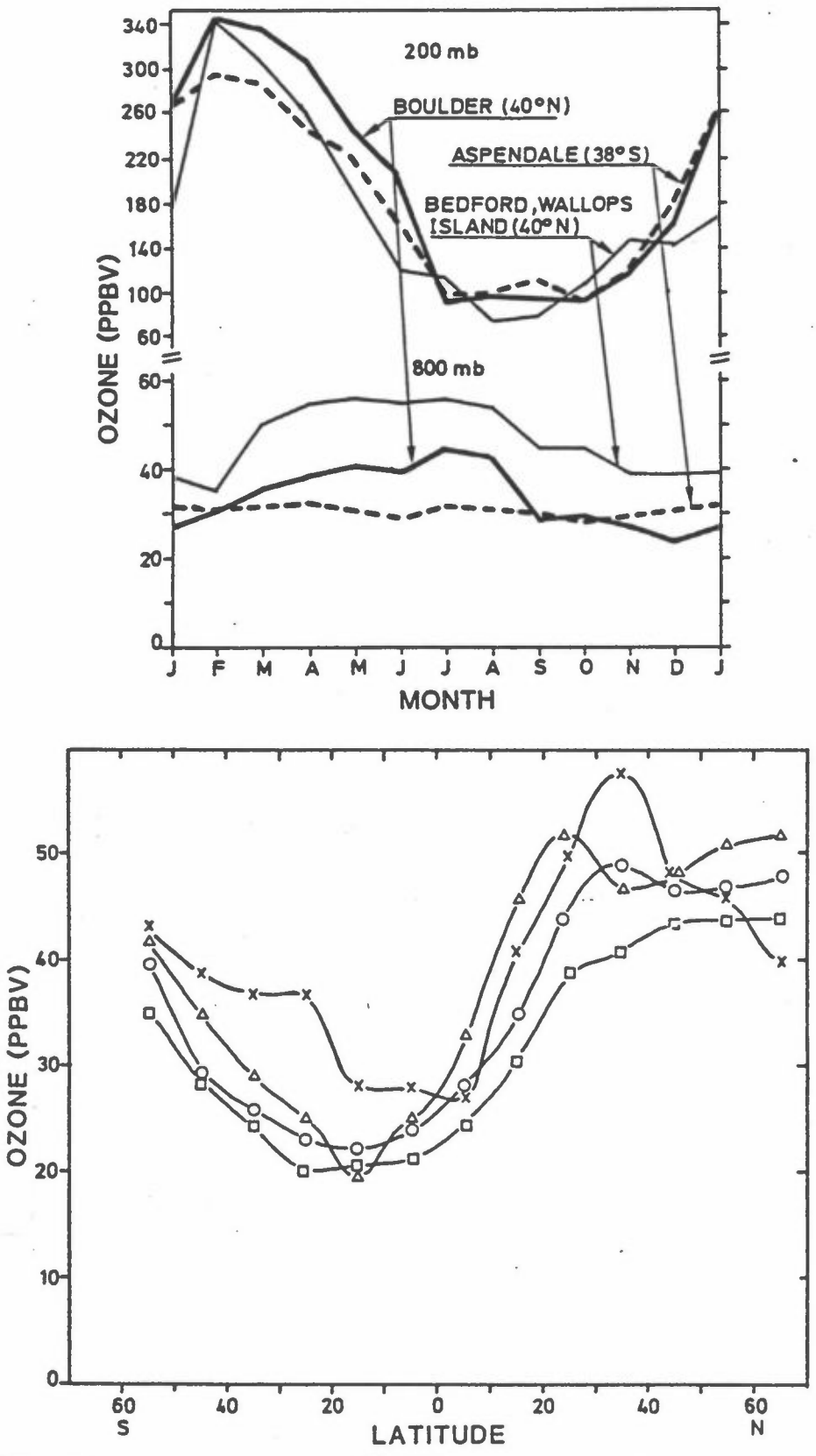

Figure 8: (Upper part) Monthly variation of the concentration of ozone at 200 mb and 800 mb at Boulder (40° N), the combined data from Bedford (42° N) and Wallops Island (38° N) and from Aspendale (48° S) (30).
(Lower part) Measured latitudinal distribution of ozone as compiled by Seiler and Fishman (29). Open quadrates denote the tropospheric average obtained in the flights described in (29), open triangles 480 mb, outbound leg, open circles 480 mb, homebound leg (29), crosses ref. (27).

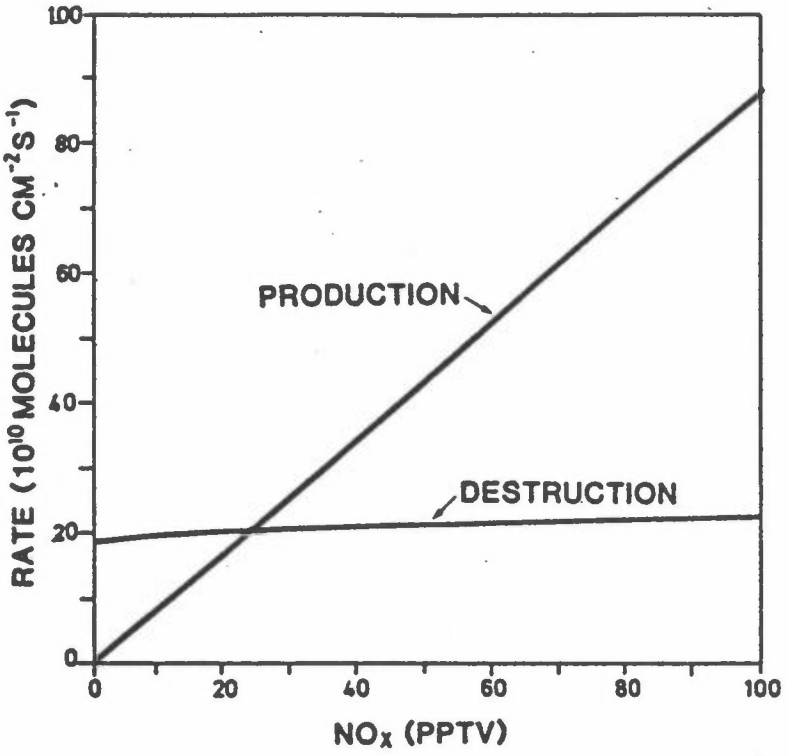

Figure 9: Calculated Northern Hemispheric average, annual mean production and destruction rates of tropospheric ozone as a function of average NO_x concentration (30).